Virchows Arch A [Pathol Anat] (1986) 410:31–42

Virchows Archiv A

Ultrastructure, renin status, contractile and electrophysiological properties of the afferent glomerular arteriole in the rat hydronephrotic kidney *

Rainer Nobiling [1], Christian P. Bührle [1], Eberhard Hackenthal [2], Udo Helmchen [3], Michael Steinhausen [1], Andrea Whalley [1], and Roland Taugner [1]

[1] I. Physiologisches Institut und [2] Pharmakologisches Institut der Universität Heidelberg, Im Neuenheimer Feld 326/366, D-6900 Heidelberg

[3] Pathologisches Institut der Universität Göttingen, Robert-Koch-Strasse 40, D-3400 Göttingen, Federal Republic of Germany

Summary. Histological, ultrastructural, immunohistochemical, intravital microscopic and electrophysiological techniques have been applied to study experimental hydronephrosis in rats in order to assess its value as a preparation for the investigation of renal microcirculation and of the electrophysiological properties of the renin-containing juxtaglomerular (JG) cells of the afferent glomerular arteriole.

As hydronephrosis develops, the kidney parenchyma becomes progressively thinner owing to tubular atrophy. Twelve weeks after ureteral ligature, this process results in a transparent tissue sheet of about 150–200 μm in thickness. In this preparation, the renal arterial tree as well as the glomeruli can be easily visualized for intravital microscopic studies, e.g. the determination of kidney vessel diameters, or the identification of JG cells for penetration with an intracellular microelectrode. In contrast to the tubular atrophy, the vascular system is well preserved, and the JG cells and the sympathetic axon terminals are ultrastructurally intact. This is also true for the glomeruli, except for a certain confluence of the podocyte foot processes and a thickening of the basal laminae. Renin immunostaining and kidney renin content in the hydronephrotic organ correspond to those in control kidneys. In addition, there are no differences in the plasma renin levels of hydronephrotic and control rats.

Intravital microscopic observations reveal that the renal vascular tree reacts in a typical, concentration dependent manner to the vasoconstrictor agent angiotensin II, mainly at the level of the resistance vessels. Electrophysiological recordings from juxtaglomerular granulated cells show a high membrane potential (−60 mV), and spontaneous depolarizing junction potentials, owing to random transmitter release from the nerve terminals. Angiotensin II, an inhibitor of renin release, depolarizes JG cells reversibly.

Hence, we may infer that the hydronephrotic rat kidney is a suitable model for in vivo studies of the renal microcirculation as well as for in vitro investigations of the electrophysiological properties of the media cells of the afferent glomerular arteriole.

Key words: Hydronephrotic kidney – Renin-angiotensin system – Microcirculation of the kidney – Juxtaglomerular cells

Introduction

Recent experiments indicate that hydronephrotic kidneys of both rats and mice are versatile models for in vivo and in vitro studies of the renal vasculature including direct microscopical observation of glomerular microcirculation (Steinhausen et al.

* This work was supported by the Deutsche Forschungsgemeinschaft within the Sonderforschungsbereich 90 'Cardiovaskuläres System' and within the Forschergruppe Niere/Heidelberg

Offprint requests to: R. Taugner at the above address

1983), or electrophysiological recordings from juxtaglomerular granulated cells and vascular smooth muscle cells (Bührle et al. 1985). In the intact kidney and in kidney slices, the microvessels, glomeruli and juxtaglomerular granulated cells cannot be observed directly with a microscope, nor manipulated experimentally, since they are embedded in the vast cellular mass of tubular epithelium. After prolonged ureteral obstruction with and without preceding renal ischaemia the situation is different. As a consequence of this procedure, the tubular system is subject to atrophy, leaving only the vascular structure intact, embedded in a fibrous tissue sheet of 150–400 μm thickness. Thus, the hydronephrotic kidney preparation offers distinct advantages over intact kidneys or kidney slices: The tissue is very thin and transparent, permitting microscopic observation of the glomerular microcirculation in transmitted light (Steinhausen et al. 1983, 1985). In addition, the diffusion paths in such preparations are short, so that a sufficient oxygen supply can be provided in vitro by superfusion of the tissue, e.g. for intracellular recordings from juxtaglomerular granulated cells (Bührle et al. 1984, 1985, 1986a).

As a basis for future work, we have determined the renin content and localization in hydronephrotic kidneys and assessed – on morphological grounds – the integrity of renal resistance vessels, epithelioid cells, glomeruli, and sympathetic innervation. Furthermore, first intracellular recordings from rat juxtaglomerular epithelioid cells and also in vivo intravital microscopic findings relating to the response of the renal microcirculation to angiotensin II are presented.

Material and methods

Experimental hydronephrosis was induced in 37 Sprague-Dawley and 17 Wistar-Firth rats of 200–250 g body weight. Before surgery, the rats were anesthetized by intraperitoneal injection of sodium pentobarbitone (Nembutal®, 60 mg/kg). The left kidney was exposed by a flank incision, and the ureter was doubly ligated with 3–0 silk suture. In order to induce ischaemia, a small hooded bulldog clamp was placed on the renal artery and removed after 60 min. Subsequently, the incision was closed again. In some of these 200–250 g rats, hydronephrosis was induced without ischaemia for comparison purposes. In order to obtain very thin preparations for electrophysiological experiments, young rats of initially 40–60 g body weight were also used. Again, in these younger animals hydronephrosis was produced without preceding renal ischaemia.

1, 2, 4, 8 and 16 weeks after the operation, 3 of the 200–250 g rats were processed for electron microscopy, 3 for immunohistochemistry, and 2 for determination of plasma and kidney renin. Under Nembutal® anesthesia – as outlined above – the abdomen was opened by a midline incision, and the abdominal aorta was cannulated for perfusion fixation as described previously (Taugner et al. 1979, 1984b). For immunocytochemistry, the animals were perfused with Bouin's fluid without acetic acid, whereas for electron microscopy the solutions proposed by Forssmann et al. (1977) were used. Before perfusion, the dimensions of the kidneys were determined in situ.

After fixation, 1–3 mm thick slices of the kidneys were dehydrated in ethanol and embedded in paraffin. Sections of 7 μm thickness cut perpendicularly to the longitudinal axis of the kidney were reacted with anti-renin serum as described previously (Taugner et al. 1979) and processed according to the PAP-technique of Sternberger (1979). To test the immunohistochemical specificity of the reaction, the usual procedures, including immunoabsorption and incubation of the sections with preimmunesera were performed. The sections were examined and photographed with a Photomikroskop III (Carl Zeiss, Oberkochen, FRG).

Electron microscopic procedures (Epon embedding, ultrathin sectioning, and staining) were conventional and have been described earlier (Taugner et al. 1984b). The ultrathin sections were examined and photographed in an EM 10 A electron microscope (Carl Zeiss, Oberkochen, FRG) at an accelerating voltage of 60 kV. For the determination of plasma renin, blood samples of 500 μl were taken, centrifuged in a desk top centrifuge at 12.000 g and the plasma immediately frozen; hydronephrotic and control kidneys were removed from the animals and also frozen immediately. Renin was determined by radioimmunoassay of angiotensin I liberated during incubation of the samples with a rat angiotensinogen preparation (Hackenthal et al. 1983).

The intravital microscopic experiments were done 9–12 weeks after ureteral obstruction under thiobarbitone anesthesia (Inactin BYK, 100 mg/kg, i.p.) with the trachea of the animals intubated. Continuous blood pressure measurements were performed after cannulation of the left cartoid artery, whereas saline (0.06 ml/min) was permanently infused through a left jugular vein cathether. After a flank incision, the left, hydronephrotic, kidney was exposed and split by cautery along its greater curvature. Subsequently, the dorsal half of the kidney was sutured to a kidney-shaped wire as described in detail previously (Steinhausen et al. 1983). The body temperature of the rat was maintained at 37° C by an automatic heating device, while the split kidney was placed in a tissue bath filled with isotonic, isoosmotic solution (Hämaccel) at a temperature of 37° C.

For the intravital microscopic observations, Ultropak UO-55 (1:55, 0.85) lenses (Ernst Leitz, Wetzlar, FRG) were used. All measurements of vessel diameters were performed in transmitted light, using a video camera mounted on the tube of the light microscope with the image displayed on a monitor. Angiotensin II was topically added to the tissue bath, starting at a concentration of 10^{-9} mol/l; the vessel diameters were measured 5 and 10 min after angiotensin II application. Subsequently, the bath concentration of angiotensin II was raised to 10^{-8} mol/l and, finally, to 10^{-7} mol/l and the protocol for diameter measurement was repeated accordingly. This local application of angiotensin II did not lead to changes in the systemic blood pressure.

For electrophysiological experiments, hydronephrotic rats with an initial body weight of 40–60 g were used. Under pentobarbitone sodium (Nembutal®, 50 mg/kg, i.p.) anesthesia, the kidneys were rinsed free of blood with Tyrode's solution in situ via a catheter in the abdominal aorta and subsequently injected with a suspension of washed india ink particles in order to make the renal vasculature clearly visible. The kidneys were decapsulated, removed from the animals, and mounted in a concentric tissue holder of 4 mm inner diameter to give a plane sheet of a thickness not exceeding 150 μm. The tissue holder was then transferred to the recording chamber and continuously superfused with oxygenated Tyrode's solution (pH = 7.4; tem-

perature = 37° C) at a rate of 6 ml/min. The translucent tissue was illuminated from below and viewed from above with a compound microscope equipped with a water immersion lens (Ernst Leitz, Wetzlar, FRG; 1:22, 0.45) at a final magnification of 275. The juxtaglomerular granulated cells were impaled with conventional single-barrelled microelectrodes of the filament type with the aid of a remote controlled, step motor driven micromanipulator (Marcinowski, Heidelberg, FRG) as described previously (Bührle et al. 1985). When filled with 3 mol/l potassium acetate, the electrodes had resistances in excess of 120 MOhm. They were connected to the input stage of a high impedance, capacitance compensated amplifier (Axoclamp 2, Axon Instruments, Burlinggame, Mass., USA) via $Ag/AgCl_2$ wires. The membrane potential was displayed on a digital oscilloscope (Iwatsu 6440) and recorded on a potentiometric writing system. Pharmacological agents were applied by superfusion in the bath solution. JG cells were identified on a microtopographical basis as described earlier.

Results

The changes of the kidney after ischaemia and ureteral ligation (UL) are characterized by a progressive increase in the size of the organ. A maximum was reached – in rats with postischaemic hydronephrosis – about 8 weeks after UL, and kidney dimensions then rather decreased than increased (Fig. 1A). Generally, atrophy started from the perihilar region and spread towards the circumference of the organ. First, the medulla was affected, and subsequently also the renal cortex was involved. In uncomplicated cases the fluid within the renal pelvis was clear, sometimes, however, haemorrhagic or purulent fluid was found.

As soon as one week after UL the kidney was distinctly enlarged, the pelvis distended, and the ureter dilated. Compared with controls, the rim of the parenchyma was thinned by medullary atrophy, with the size of the papilla being considerably reduced. Two weeks after UL, the length and width of the kidney were increased nearly twofold as compared to controls. The pelvis was markedly distended and there was further thinning of the parenchyma, caused by progressive medullary atrophy. The papilla was again reduced in length. The renal cortex remained largely unaffected (Fig. 2A).

Four weeks after UL, concomitant with a further increase in the size of the organ, the atrophy of the renal cortex became obvious. The blunt papilla was now barely visible (Fig. 2B). Eight weeks after UL, the kidney attained a more spherical shape. The width of the parenchyma was now reduced to 150–400 µm. Organs where neither haemorrhage nor intrapelvic suppuration had occurred were translucent. Some of them showed radial segmentation by the interlobar arteries. Sixteen weeks after UL there were little changes in gross appearance when compared with kidneys 8 weeks after UL.

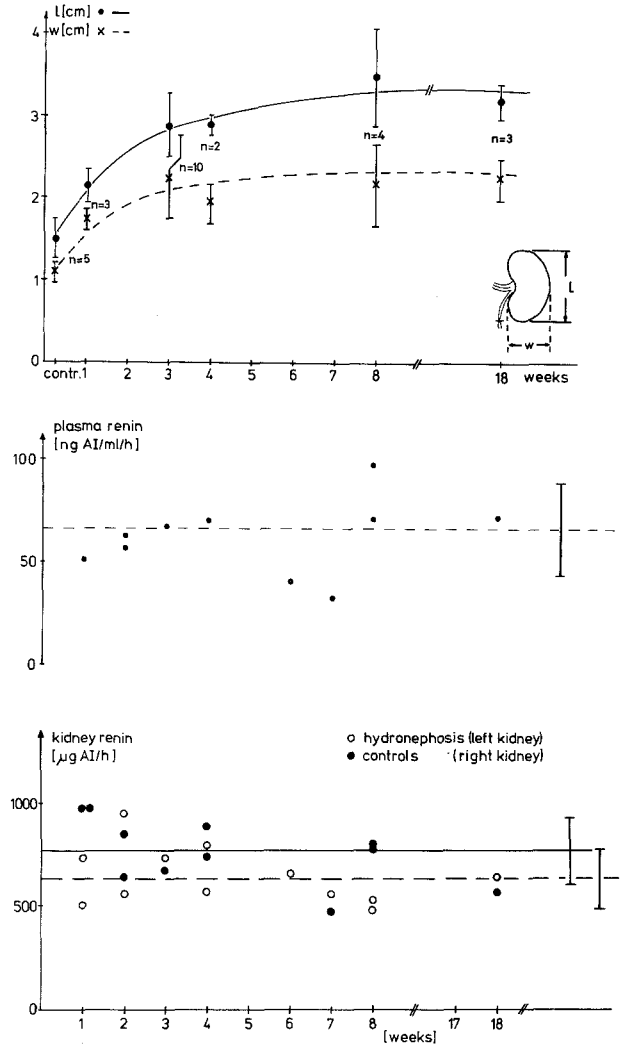

Fig. 1. *Upper panel (A):* Dimensions of rat hydronephrotic kidneys during development of hydronephrosis. Both width and length of the kidneys increase up to the eigth week after ureteral obstruction and remain stationary thereafter. *Middle panel (B):* Plasma renin level in rats with experimental ureteral obstruction. This parameter remains essentially constant up to 18 weeks after surgery. *Lower panel (C):* Development of kidney renin in hydronephrotic (*open circles*) and in the contralateral control organs (*filled circles*). There is neither a significant difference between normal and hydronephrotic organs, nor does kidney renin change as the hydronephrotic process advances

In 200–250 g animals, where the renal artery had not been temporarily occluded in order to produce ischaemia, the development of hydronephrosis followed essentially the same lines, although at a somewhat slower rate; i.e. a state of hydronephrosis reached 8 weeks after UL with ischaemia would require about 12 weeks without ischaemia. Although the time course of progressive hydronephrosis was not studied in the 40–60 g rats, the

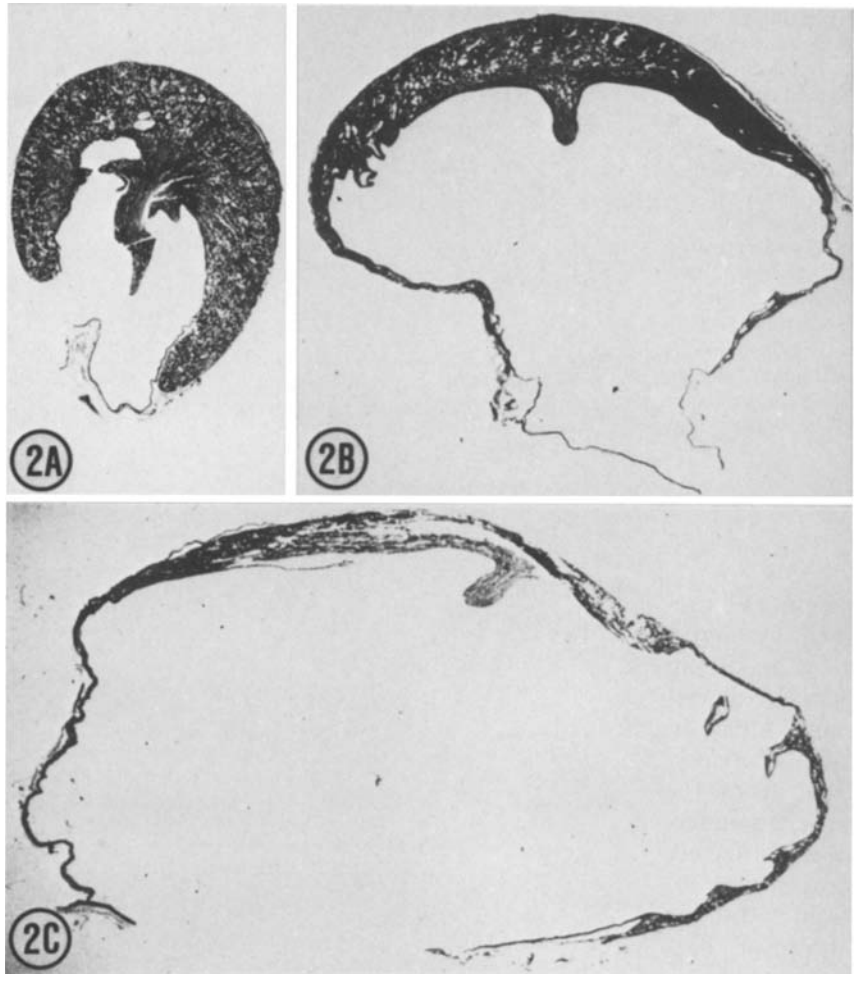

Fig. 2. Reduction in parenchymal thickness in rat kidney 1 week (**A**), 2 weeks (**B**), and 4 weeks (**C**) after experimental ureteral obstruction. The atrophy of the parenchyma involves first the perihilar region, and then proceeds towards the circumference. Note the persistence of the renal papilla (Masson-Goldner stain, 5,5×)

final stage was characterized by a particularly thin residual parenchyma not exceeding 150 μm, making these organs very suitable for electrophysiological experiments where high translucency was of prime importance.

Since in hydronephrotic kidneys the glomeruli had been displaced from their normal three-dimensional arrangement to a nearly two-dimensional array, in paraffin sections they appeared to be more densely packed than glomeruli from control organs. With respect to immunostaining, hydronephrotic tissue corresponded to tissue taken from control kidneys: After reaction with anti-renin serum and processing according to the PAP-technique, virtually all afferent vessels in hydronephrotic tissue were positively immunostained (Fig. 4B), the renin-positive parts of these vessels extending up to 80 μm upstream from the points of entry of the afferent arterioles into the glomeruli. Hence, the localization of the renin-positive, i.e. epithelioid, cells corresponds to that observed in controls (cf. Taugner et al. 1984a). In addition, the renin content of the individual cells as judged on the basis of the intensity of the reaction at equal dilutions of the anti-renin serum, appears to be comparable to that in untreated kidneys. There was no change in immunoreactivity and percentage of renin-positive afferent vessels in the course of the development of hydronephrosis. As in the epithelioid cells of control kidneys, so in those of hydronephrotic organs angiotensin II was found to coexist with renin (Fig. 4C).

The renin content of hydronephrotic and untreated contralateral organs 1–16 weeks after UL is shown in Fig. 1C; it is evident that there is no detectable trend in the renin content during the progression of hydronephrosis. The same is true for the plasma renin activity which is displayed in Fig. 1B. In the contralateral, untreated kidneys, mean renin content was 763 ± 163 μg ANG I/60 min ($n=11$), whereas in the hydronephrotic organs 631 ± 147 μg ANG I/60 min were found ($n=12$). The difference between both groups was not statistically significant.

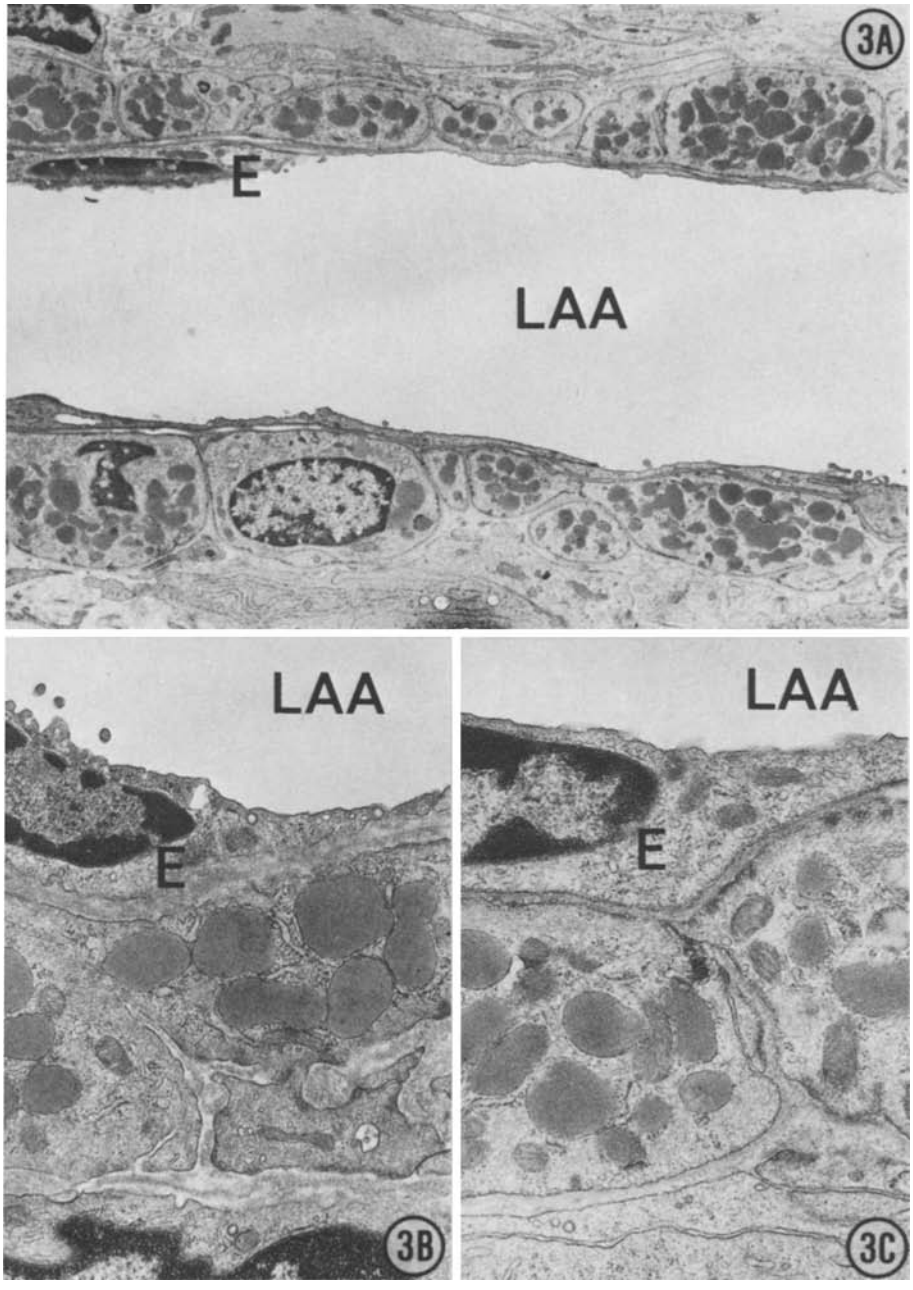

Fig. 3. Epithelioid cells in the media of a rat afferent arteriole. Neither the vessel as a whole (**A**), nor individual epithelioid cells in the early (1 week, **B**) and the late (18 weeks, **C**) stage of hydronephrosis show any conspicuous morphological differences as compared to controls. *LAA:* lumen of the afferent arteriole, *E:* endothelial cell (**A** 4,900 × ; **B**, **C** 18,000 ×)

In the course of developing hydronephrosis, there were very few changes in the ultrastructure of the media of the glomerular arterioles. Up to 16 weeks after ureteral obstruction, there were neither changes in the shape of epithelioid cells, nor in the morphological aspect of their organelles. At all stages of cortical atrophy, the epithelioid cells were replete with mature, membrane bounded granules which have been shown to contain renin (Taugner et al. 1984b, d; Fig. 3). The rough endoplasmic reticulum was well developed with the ribosomes firmly adhering to the membranes. There were no signs of metabolic damage, such as mitochondrial swelling or calcification. The other organelles, such as nucleus or Golgi apparatus, were indistinguishable from those observed in control kidneys. The same holds for the vascular smooth muscle cells of the afferent vessel, which are located upstream from the epithelioid cells. Myofilaments and attachment sites were clearly distinguishable, and the organelles were unaltered when compared with controls. Frequently, axon terminals which contained clear vesicles were found in close contact with either epithelioid cells or vascu-

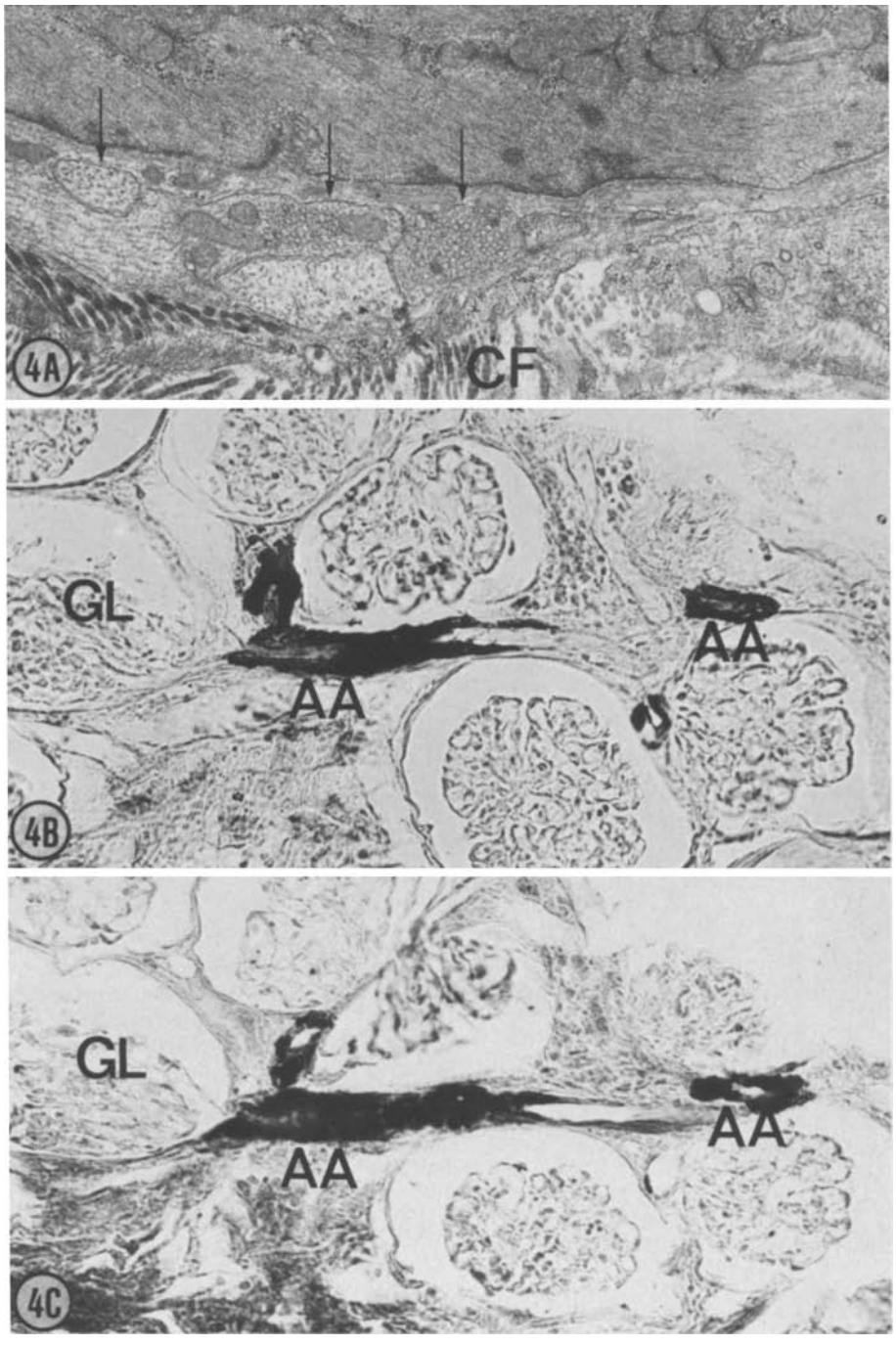

Fig. 4. A. Intact vascular smooth muscle cells and sympathetic axon terminals in the wall of an afferent arteriole 10 weeks after ureteral obstruction. The minimal distance between the axon terminals and the vascular smooth muscle cells is 150 nm in this example. Note the collagen fibrils within the adventitia of the vessel (19,900×). **B** and **C** renin and angiotensin II in serial sections taken from a hydronephrotic kidney 18 weeks after ureteral obstruction. *GL:* glomerulus, *AA:* afferent arteriole. Dilution of the antisera: 1:10,000 in **B** and 1:500 in **C**; PAP-technique (245×)

lar smooth muscle cells, the distance ranging between 80 and 300 nm (Fig. 4A). The endothelium of the renal vessels was also found to be unaltered as compared to controls (Fig. 3). On the adventitial side of the vessels, the amount of surrounding collagen fibres was greatly augmented. This deposition of collagen fibres appeared to increase during the progression of cortical atrophy.

The relative integrity of the vascular structures contrasts with the ultrastructural alterations which occurred in glomeruli, and, much more obviously in tubular epithelia. In the majority of the glomeruli, as soon as one week after ureteral obstruction, some thickening of the foot processes of the podocytes was observed. At that time, the basal lamina was not affected, and the fenestrated endothelial cells of the glomerular capillaries were apparently normal (Fig. 5A). In the overwhelming majority

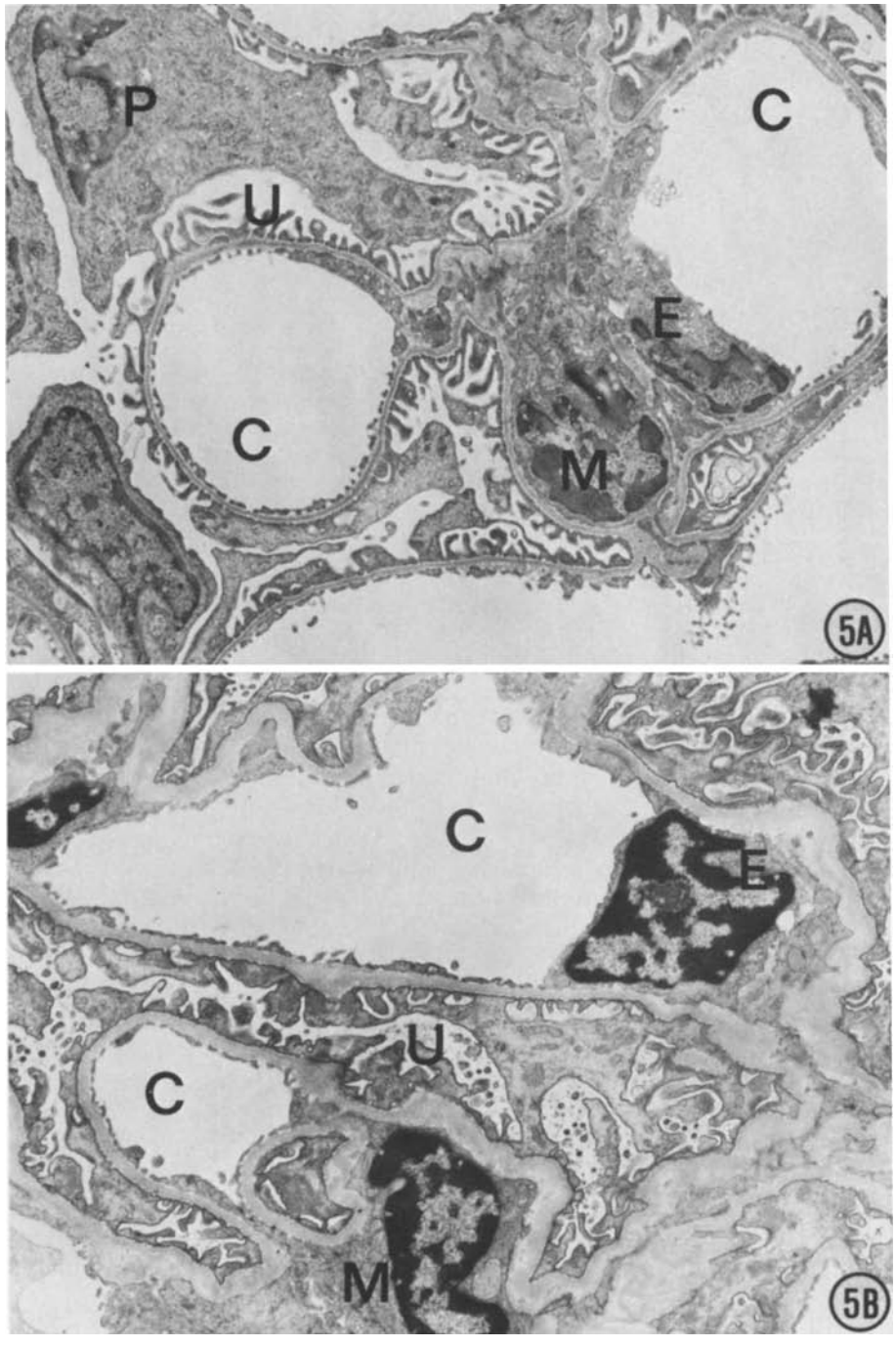

Fig. 5. Alterations in glomerular ultrastructure 1 week (**A**) and 8 weeks (**B**) after ureteral obstruction. Most prominent is the progressive reduction of the urinary space and the deformation of the capillaries during the development of hydronephrosis. The basal lamina increases in thickness, and there is marked flattening and confluence of podocyte foot processes. After 8 weeks (**B**), debris of indeterminate origin has accumulated in the urinary space. *M:* mesangial cell, *E:* endothelial cell, *C:* capillary, *P:* podocyte, *U:* urinary space (6,900 ×)

of the glomeruli, the macula densa was already altered severely, with the tubular lumen collapsed and the macula densa cells at all stages of disintegration (Fig. 6). In some cases, the macula densa could not be identified even in serial sections through the glomeruli.

In contrast with that, the adjacent Goormaghtigh cell field and the communicating glomerular stalk exhibited little signs of damage (Fig. 6).

At later stages, i.e. 2–8 weeks after UL, in the majority of glomeruli there was a marked convolution and thickening of up to 5 times its normal width of the filtration membrane's basal lamina (Fig. 5A). These changes were accompanied by a prominent deformation of the podocyte foot processes, which became increasingly confluent. In parallel, the endothelial fenestrations became quite irregular. In the course of developing hydrone-

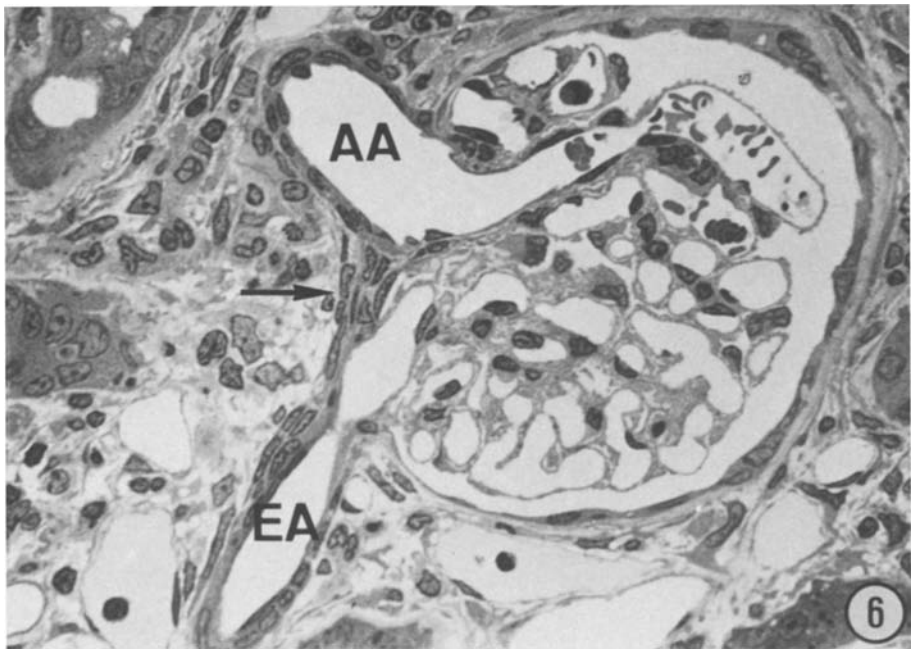

Fig. 6. Renal corpuscle 4 weeks after ureteral obstruction. After 4 weeks, the glomerulus does not appear to be severely altered. No macula densa is detectable in the angle between afferent (*AA*) and efferent (*EA*) arteriole. The Goormaghtigh cell field (arrow) is in its normal position and has been spared by the process of cortical atrophy. (Semithin section, toluidine blue stain, × 580)

phrosis, an increasing amount of debris was found in the urinary space of the glomeruli (Fig. 5B). With further progression of cortical atrophy, the urinary space tended to collapse, and the glomerular capillaries which showed a round profile one week after ureteral obstruction, became polygonal.

It is, however, noteworthy that at a certain stage of the development of hydronephrosis the glomeruli were not damaged to an equal extent. In extreme cases, there would be nearly intact glomeruli in the immediate vicinity of glomeruli whose Bowman capsule had been entirely disrupted, i.e. where the urinary space communicated freely with the extracellular space of the renal cortex.

In order to determine the vasoconstrictor response at different levels of the renal vascular tree to angiotensin II, this compound was applied in the bath solution of the split hydronephrotic kidney and the vessel diameters measured as described in 'methods'. Application of angiotensin II produced a significant and concentration-dependent vasoconstriction, predominantly in the pre- and postglomerular arterioles, whereas the larger vessels were affected to a lesser extent. Table 1 summarizes the results of these experiments. Examples of the reactions of an interlobular artery and two afferent arterioles after i.v. infusion of angiotensin II are displayed in Fig. 7A, B.

Impalement of JG cells with intracellular microelectrodes was indicated by a sudden negative deflection of the potential recording. At rest, the membrane potential in rat JG cells was 59.1 ± 12.1 mV ($n = 19$). The JG cells exhibited spontaneous, random depolarizations of up to 10 mV amplitude, (noise level of the recording system approx. 0.4 mV) occurring at frequencies between 40 and 100 min^{-1} (Fig. 8, inset). These spontaneous depolarizing events were quite similar to those observed in JG cells of the hydronephrotic mouse kidney (Bührle et al. 1985; 1986a, b).

Occasionally, stable recordings lasting up to 2 h were obtained that permitted to test the actions of pharmacological agents upon the membrane potential. Angiotensin II which strongly inhibits renin secretion, reversibly depolarized the JG cells. The liminal concentration for a detectable membrane potential effect was 10^{-9} mol/l. This depolarization was accompanied by an increase in frequency and amplitude of the spontaneous depolarizing junctional events, i.e. by a facilitation of junctional transmission, as already observed in mouse JG cells (Bührle et al. 1986b; Fig. 8).

Discussion

The macroscopic changes in kidney morphology which we observed in rats after unilateral ureteral ligation resembled those reported for various species, e.g. guinea pigs (Holle and Schneider 1961), rats (Endes et al. 1962; Kelemen and Endes 1965), and rabbits (Rao and Heptinstall 1968; Hinman 1934, 1945a, b, c). Earlier observations indicate that the residual thickness of the renal cortex after long-lasting ureteral obstruction varies considera-

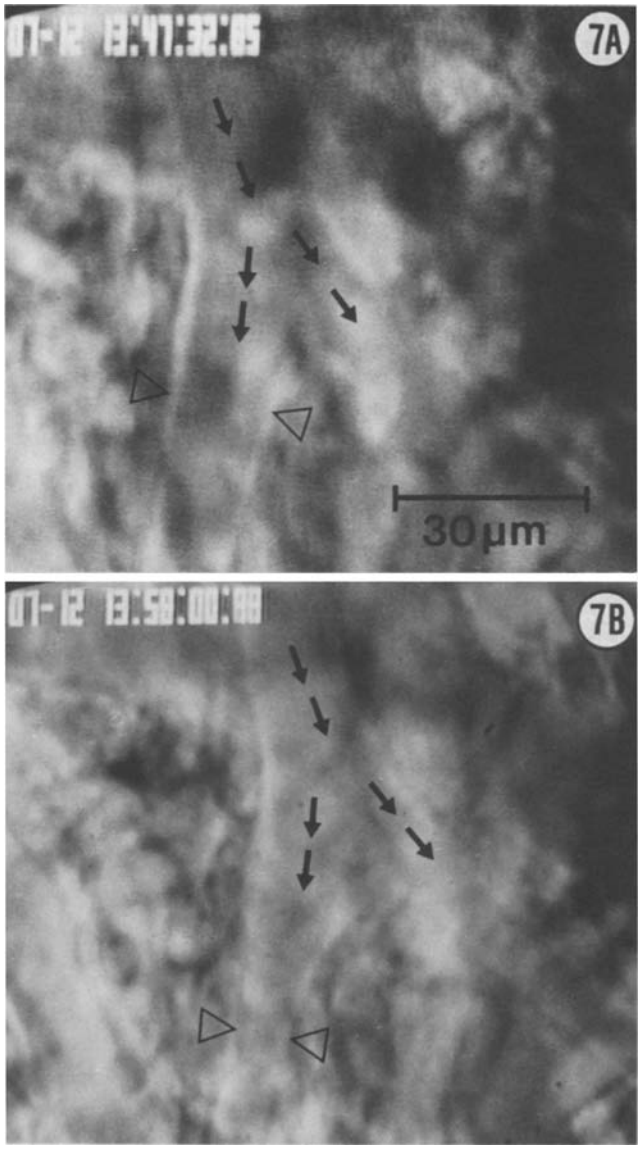

Fig. 7. In vivo photomicrogram of the branching of an interlobular artery into two afferent arterioles in the split hydronephrotic kidney of the rat under control conditions (**A**), and after i.v. infusion of 50 ng angiotensin II/kg·min (**B**)

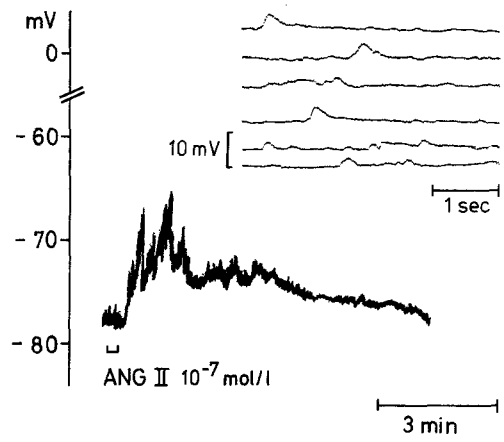

Fig. 8. Depolarizing action of angiotensin II upon a juxtaglomerular granulated cell in the afferent arteriole of the isolated rat hydronephrotic preparation. A 15s application of 10^{-7} mol/l angiotensin II reversibly depolarizes the cell from −78 mV to approx. −68 mV; this depolarization is accompanied by an increase of both frequency and amplitude of the spontaneously occurring junction potentials, indicating faciliation of junctional transmission. *Inset:* junction potentials on a faster time scale, measured at the maximum of the ANG II-induced depolarization

Table 1. Changes of luminal diameters after local application of Angiotensin II in percent of control values

	Angiotensin II-bath concentration		
	10^{-9} M	10^{-8} M	10^{-7} M
Aa. arcuatae proximal	95,8 ±2,7	91,4 ±4,4	71,8 ±9,7*
Aa. arcuatae distal	95,1 ±3,8	91,2 ±2,9*	78,0 ±4,5*
Aa. interlobulares	94,9 ±5,6	90,6 ±4,2	60,7 ±7,1*
Vasa afferentia (near Aa. interlobulares)	98,4 ±4,1	89,9 ±9,8	65,5 ±5,3*
Vasa afferentia (near glomeruli)	92,7 ±6,2	74,3 ±8,7*	62,7 ±6,3*
Vasa efferentia (near glomeruli)	90,9 ±5,8	83,4 ±8,6	66,8 ±9,1*
Welling points	94,7 ±1,1	90,8 ±1,7	89,6 ±2,1

* $= p < 0{,}05$ $n = 8$

bly between different species. Apparently, in smaller species the remaining parenchyma is thinner than in larger ones, although at equal values of filtration pressure, according to Laplace's law, wall tension should be higher in larger kidneys than in smaller ones (cf. Wyker et al. 1981). This, however, may be attributed to differences in content and mechanical properties of connective tissues of various species. Transient ischaemia appeared only to accelerate the development of hydronephrosis, without causing any detectable qualitative morphological changes, i.e. minimal cortical thickness would be reached in 8–10 weeks compared to 12–16 weeks in animals in which the renal artery had not been clamped.

However, in young rats of initially 40–60 g b.w. ureteral ligation led to a much more pronounced hydronephrosis after a comparable period of time than in rats with an initial b.w. of 200–250 g. Whether this is due to a greater content of connec-

tive tissue in kidneys of adult rats as opposed to younger animals is not clear.

In the present study, the structure and ultrastructure of the renal vasculature, including the glomeruli, was examined in order to provide a morphological basis for recent work on glomerular microcirculation already published, and extended in this paper (Steinhausen et al. 1983). In addition, we have focussed our interest on the juxtaglomerular apparatus, and in particular, on the morphology of epithelioid cells and vascular smooth muscle cells, since we intend to use the rat hydronephrotic kidney as a model preparation for more extensive electrophysiological and biochemical investigations of the renin-angiotensin system.

In contrast with the tubular epithelia, atrophy of which may partly be the result of hypoxia as well as of inactivity as a consequence of decreasing and/or stopped filtration (Taugner et al., unpublished work) the mesenchymal elements in the cortex of the hydronephrotic kidney, that is to say, the vascular smooth muscle cells, epithelioid cells, and endothelial cells, were affected very little. Glomerular mesangial cells and podocytes, however, were altered morphologically without showing signs of necrosis. Even intact sympathetic axon terminals, usually considered rather susceptible to pressure-induced damage, were regularly found. Whether the resistance to atrophy of cells within and adjacent to the media of blood vessels rests on the short diffusion path between lumen and wall of microvessels, on a protective role of the connective tissue within the vessel wall, or on an inherently greater resistance of the cells to stress-induced alterations is still unclear.

In excitable as well as in inexcitable cells, the resting membrane potential may be taken as a fast and sensitive indicator for mechanical, metabolic or toxic damages inflicted on the cells (Cohen and DeWeer 1977). In the hydronephrotic rat preparation, the membrane potential of the JG cells was higher than that measured in most comparable preparations, e.g. in the rat tail artery (Cheung 1982), the guinea pig ear artery (Kajiwara et al. 1981), or in guinea pig mesenteric arterioles (Takata 1980). This is strong support for the assumption that the active ion transport systems of the JG cells which are responsible for the maintenance of the transmembrane ion activity gradients and, consequently, of the membrane potential, are still operative in the hydronephrotic preparation. Hence we may infer that the JG cells in the media of the afferent glomerular arteriole in the hydronephrotic rat kidney are not in an inferior condition as compared to VSM cells in other commonly used in vitro preparations. In addition, the reversible depolarizing response of the JG cells to angiotensin II indicates the presence of specific membrane receptors for this compound that are linked to receptor operated membrane channels (cf. Bolton 1979). Although not analyzed in detail, the occurrence of spontaneous random depolarizations which closely correspond to similar events observed in our experiments in the mouse kidney as well as to spontaneous excitatory junction potentials found in a variety of smooth muscle preparations (Hirst and Neild 1978; Cheung 1982) provide strong evidence that the sympathetic axon terminals innervating these cells are still functionally intact and able to release transmitter. Correspondingly, the studies of glomerular microcirculation described earlier demonstrate that glomerular blood flow in the hydronephrotic preparation shows no conspicuous deviation from that observed in control kidneys (Steinhausen et al. 1983). In addition, afferent and efferent arterioles are still susceptible to the effects of vasoconstrictor and vasodilator agents.

It is of particular significance that this preparation is quite suitable for measurement of kidney vessel diameters at virtually all levels of the vascular tree under controlled experimental conditions. With bath application, exact concentrations of the vasoactive agent to be tested can be given to the regions of interest, with the compound acting from the adventitial side upon the vessel, i.e. with only minor interferences by the endothelium. In contrast, with systemic administration, the concentration dependence of the observed phenomena may be obscured by concentration differences at various levels of the vascular tree and/or by endothelium-mediated effects.

The findings obtained with angiotensin II suggest that vasoconstriction in the kidney – at equal concentrations – mainly occurs at the level of the resistance vessels, whereas the arcuate arteries react to a lesser extent. It is noteworthy, that the degree of vasoconstriction evoked by locally applied angiotensin II is nearly as pronounced in the efferent as in the afferent vessel, although the wall of the postglomerular arteriole consists of pericyte-like cells as opposed to the regular vascular smooth muscle cells forming the media of the preglomerular arteriole. However, the media cells of the rat efferent vessel have recently been shown to contain an appreciable amount of myosin as a prerequisite for contraction with immunohistochemical techniques (Taugner et al., unpublished work).

With systemic application of angiotensin II, preferential efferent vasoconstrictor effects of cir-

culating angiotensin II have been reported. This shift of predominance from afferent to efferent contraction may be attributed to the close proximity of the efferent vessels to the fenestrated peritubular capillaries and to the particular character of the endo-endothelial junctions which have to be considered to be more permeable to the blood-borne angiotensin II at this site (cf. Mink et al. 1984). Under physiological conditions, locally produced angiotensin II has also to be considered, being cleaved in the kidney interstitium from its precursors, and there is the contention that this peptide, in very high concentrations in the peritubular capillaries (cf. Navar and Rosivall 1984) accentuates the preferential vasoconstriction of the efferent arteriole, to maintain filtration pressure (cf. Handa and Johns 1985; Hall et al. 1977).

The viability of the vascular structures in the hydronephrotic organ is also reflected in the capability of epithelioid cells to synthesize and secrete renin under these conditions. The ultrastructural findings of unaltered granules and an intact rough endoplasmic reticulum are complemented by the immunohistochemical demonstration of renin and by the biochemical determination of total renin content which does not differ from that in the contralateral or in control kidneys. Supporting evidence for the functional integrity of epithelioid cells is provided by observations in the isolated perfused hydronephrotic rat kidney (Hackenthal et al., unpublished work), where renin secretion was influenced in a typical manner by a series of well known stimulators, e.g. isoproterenol, and inhibitors, e.g. angiotensin II. In this context, it is noteworthy that the total renin content of the hydronephrotic kidney is not significantly different from that of the contralateral organ or of control kidneys in animals without hydronephrosis. Together with the observation that the plasma renin level in hydronephrotic animals corresponds to that in normal rats, this would indicate that renin synthesis and release are in a steady state comparable to that obtaining under normal conditions, since an increased renin synthesis in the hydronephrotic kidney would tend to decrease the renin content of the contralateral kidney, while a decreased synthesis would have the opposite effect (cf. Taugner et al. 1983; Bührle et al. 1984). The question remains whether in the hydronephrotic kidney the epithelioid cells operate under conditions different from those obtaining in normal organs. Our results provide strong indications for the ability of the sympathetic axons to conduct impulses, and for a release of transmitter from the terminals (cf. Bührle et al. 1985). Since the endothelium is intact and the general structure of the afferent vessel appears to be unchanged, we have to infer that the mechanoreceptor mechanism which has been ascribed to myoendothelial junctions (Taugner et al. 1984c) is also still operative. The macula densa signal of the tubulo-glomerular feedback mechanism, however, is certainly absent, since the macula is destroyed in the course of tubular atrophy. Hence, the epithelioid cells, although morphologically intact, work under unknown conditions of stimulation in hydronephrotic kidneys.

Taken together, the results of the present study indicate that the hydronephrotic rat kidney is a preparation in which the structure of the renal blood vessels, in particular of the glomerular arterioles, is virtually unaltered. This is also true for the ultrastructure of the renin-containing epithelioid cells and of the vascular smooth muscle cells, so that the hydronephrotic rat kidney appears to be a suitable preparation for microcirculation studies, especially when the renin-angiotensin system is concerned. In such investigations, it will have to be taken into account that both the mechanoreceptor mechanism and the innervation governing renin secretion are still intact, whereas the tubulo-glomerular feedback is absent owing to the filtration stop and the destruction of the macula densa. This interruption of tubulo-glomerular feedback may, however, be favourable for particular types of investigations, as has been shown by Davis et al. (1972) in the non-filtering kidney of the dog.

Acknowledgements. The expert technical assistance of Mrs. Gerda Reb and Mrs. Maria Harlacher is gratefully acknowledged. We are greatly indebted to Mrs. Martha Wybraniec for help with the preparation of the manuscript.

References

Bolton TB (1979) Mechanisms of action of transmitters and other substances on smooth muscle. Physiol Rev 59:607–688

Bührle ChPh, Nobiling R, Mannek E, Schneider D, Hackenthal E, Taugner R (1984) The afferent glomerular arteriole: Immunocytochemical and electrophysiological investigations. J Cardiovasc Pharmacol 6:S383–S393

Bührle CP, Nobiling R, Taugner R (1985) Intracellular recordings from renin-positive cells of the afferent glomerular arteriole. Am J Physiol 249:F272–F281

Bührle CP, Scholz H, Hackenthal E, Nobiling R, Taugner R (1986a) Epithelioid cells: Membrane potential changes induced by substances influencing renin secretion. Mol Cell Endocrinol 45:37

Bührle CP, Scholz H, Nobiling R, Taugner R (1986b) Junctional transmission in renin-containing and smooth muscle cells of the afferent arteriole. Pflügers Arch 406:578–586

Cheung DW (1982) Spontaneous and evoked excitatory junction potentials in rat tail arteries. J Physiol (Lond) 328:449–459

Cohen LB, DeWeer P (1977) Structural and metabolic processes directly related to action potential propagation. In: Kandel ER (ed) Handbook of physiology Section 1: the nervous system, Vol 1: cellular biology of neurons, Part 1. Am Physiol Society, Bethesda, Maryland, pp 137–159

Davis JO, Blaine EH, Witty RT, Johnson JA, Shade RE, Braverman B (1972) The control of renin release in the nonfiltering kidney. In: Assaykeen TA (ed) Control of renin secretion: advances in experimental & biology series, vol 17. Plenum Press, New York, pp 117–129

Endes P, Dévényi I, Gomba Sz (1962) Experimentelle Beeinflussung der granulierten Zellen des juxtaglomerulären Apparates durch Heminephrektomie und bilaterale Ureterligatur. Virchows Arch [Pathol Anat] 336:40–45

Forssmann WG, Ito S, Weihe E, Aoki A, Dym M, Fawcett DW (1977) An improved perfusion fixation method for the testis. Anat Rec 188:307–314

Hackenthal E, Schwertschlag U, Taugner R (1983) Cellular mechanisms of renin release. Clin Exp Hypertens A5(7, 8):975–993

Hall JE, Guyton AC, Jackson TE, Coleman TG, Lohmeier TE, Trippodo NC (1977) Control of glomerular filtration rate by renin-angiotensin system. Am J Physiol 233:F366–F372

Handa RK, Johns EJ (1985) Interaction of the renin-angiotensin system and the renal nerves in the regulation of rat kidney function. J Physiol (Lond) 369:311–321

Hinman F (1934) The pathogenesis of hydronephrosis. Surg Gynecol Obstet 58:356–376

Hinman F (1945a) Hydronephrosis. I. The structural changes. Surgery 17:816–835

Hinman F (1945b) Hydronephrosis. II. The functional changes. Surgery 17:836–845

Hinman F (1945c) Hydronephrosis. III. Hydronephrosis and hypertension. Surgery 17:845–849

Hirst GDS, Neild TO (1978) An analysis of excitatory junction potentials recorded from arterioles. J Physiol (Lond) 280:87–104

Holle G, Schneider HJ (1961) Über das Verhalten der Nierengefäße bei einseitiger experimenteller Hydronephrose. Virchows Arch [Pathol Anat] 334:475–488

Kajiwara M, Kitamura K, Kuriyama H (1981) Neuromuscular transmission and smooth muscle membrane properties in the guinea-pig ear artery. J Physiol 315:283–302

Kelemen JT, Endes P (1965) Die juxtaglomerulären granulierten Zellen bei einseitiger Hydronephrose der Ratte. Virchows Arch [Pathol Anat] 339:301–303

Mink D, Schiller A, Kriz W, Taugner R (1984) Interendothelial junctions in kidney vessels. Cell Tissue Res 236:567–576

Navar LG, Rosivall L (1984) Contribution of the renin-angiotensin system to the control of intrarenal hemodynamics. Kidney Int 25:857–868

Rao NR, Heptinstall RH (1968) Experimental hydronephrosis: A microangiographic study. Invest Urol 6:183–204

Steinhausen M, Snoei H, Parekh N, Baker R, Johnson PC (1983) Hydronephrosis: A new method to visualize vas afferens, efferens, and glomerular network. Kidney Int 23:794–806

Sternberger LA (1979) Immunocytochemistry. 2nd ed, John Wiley, New York

Takata Y (1980) Regional differences in electrical and mechanical properties of guinea-pig mesenteric vessels. Jpn J Physiol 30:709–728

Taugner Ch, Poulsen K, Hackenthal E, Taugner R (1979) Immunocytochemical localization of renin in mouse kidney. Histochemistry 62:19–27

Taugner R, Bührle ChPh, Ganten D, Hackenthal E, Hardegg Ch, Hardegg G, Nobiling R (1983) Immunohistochemistry of the renin-angiotensin-system in the kidney. Clin Exper Hypertens-Theory Practice A5(7, 8):1163–1177

Taugner R, Bührle CP, Hackenthal E, Mannek E, Nobiling R (1984a) Morphology of the juxtaglomerular apparatus and secretory mechanisms. Contr Nephrol 43:76–101

Taugner R, Bührle ChPh, Nobiling R (1984b) Ultrastructural changes associated with renin secretion from the juxtaglomerular apparatus of mice. Cell Tissue Res 237:459–472

Taugner R, Kirchheim H, Forssmann WG (1984c) Myoendothelial contacts in glomerular arterioles and in renal interlobular arteries of rat, mouse and *Tupaia belangeri*. Cell Tissue Res 235:319–325

Taugner R, Mannek E, Nobiling R, Bührle CP, Hackenthal E, Ganten D, Inagami T, Schröder H (1984d) Coexistence of renin and angiotensin II in epitheloid cell secretory granules of rat kidney. Histochemistry 81:39–45

Wyker AT, Ritter RC, Marion DN, Gillenwater JY (1981) Mechanical factors and tissue stresses in chronic hydronephrosis. Invest Urol 18:430–436

Accepted July 23, 1986